Long-Cavity Fabry–Perot Laser Amplifier Transmitter With Enhanced Injection-Locking Bandwidth for WDM-PON Application

Gong-Ru Lin, *Senior Member, IEEE*, Yu-Sheng Liao, Yu-Chieh Chi, Hao-Chung Kuo, *Senior Member, IEEE*, Gong-Cheng Lin, Hai-Lin Wang, and Yung-Jui Chen, *Fellow, IEEE*

***Abstract*—We simulate the injection-locking performance of a 1% antireflection coated Fabry–Perot laser amplifier (AR-FPLA) and demonstrate the 2.5-Gbit/s DWDM-PON application with the directly modulated AR-FPLA based ONU transmitter under side-mode injection-locking condition. The effect of the AR-FPLA front-facet reflectivity on the injection locking range detuning and the Q-factor are interpreted from theoretical simulations and are experimentally characterized. A 25-channel locking capacity is reported for such a side-mode injection-locked AR-FPLA with corresponding wavelength locking range of 30 nm, the minimal requested power of -7 dBm and gain extinction ratio of < 7 dB by reducing its front-facet reflectivity to 1%. At bit rate of 2.5 Gbit/s, the BER of 10^{-12} is achievable for the nearest 17 channels of AR-FPLA at receiving power of -21 dBm, and all of the 25 injection-locked channels with SMSR of > 35 dB can guarantee the BER of $< 10^{-9}$ with their worst receiving sensitivity degrading to -19 dBm.**

***Index Terms*—Anti-reflection (AR) coating, DWDM channelization, Fabry-Perot laser amplifier (FPLA), fiber-to-the-home, optical network unit (ONU), passive optical network (PON), side-mode injection-locking.**

I. Introduction

In next generation, the wide-area broadband access networks are required to offer high-speed connection services between the central office (CO) and remote nodes (RNs). The wavelength-division-multiplexed passive optical network (WDM-PON) is a promising candidate of the low-cost subscriber networks for the fiber-to-the-home systems due to its large capacity and flexibility. For the deployment of practical WDM-PONs, the most critical issue is to develop the low cost WDM light sources for the optical network unit (ONU). A multistage access network for bidirectional WDM transmission using AWG-sliced ASE-injected Fabry–Perot laser diode (FPLD) with simultaneous bidirectional 1.25-Gbit/s transmission per channel up to 20 km has been reported [1], [2]. The slave FPLDs used in these references were injected by an ASE light source which is sliced by an AWG based wavelength division demultiplexer. To solve the mode-selection problem, a bidirectional WDM-PON based on gain-saturated colorless reflective semiconductor optical amplifiers (RSOA) was demonstrated for 1.25-Gbit/s upstream and 2.5-Gbit/s downstream transmission over 20 km [3], [4].

One alternative approach is employing the FPLDs with single-mode output under the injection-locking with a coherent light source of a mutually injection-locked FPLD amplified by an Erbium-doped fiber amplifier (EDFA) [5], [6]. In particular, a broadband light source (BLS) emerged by mutual injection between two antireflection-coated FPLDs is used to injection-lock the FPLDs for obtaining 125-Mb/s transmission with 50-GHz channel spacing limited by the FPLD cavity length and the injection efficiency. Shin *et al.* have reported a hybrid WDM/TDM PON with each WDM channel sharing by eight subscribers to simultaneously accommodate 128 subscribers [7]. However, this method requires the complicated media access control, the high-cost burst mode receivers, and the link-bandwidth sharing. All of these achievements meet the demand of the rapidly increased capacity in the fiber-to-the-home (FTTH) communication systems based on gigabit Ethernet protocol [8]–[10]. Currently, the proposed approaches are limited by low bandwidth, power budget and high intensity noise when applying to the optical link.

In this work, we theoretically analyze and experimentally demonstrate the transmission performance of a side-mode injection-locked antireflection coated Fabry–Perot laser amplifier (AR-FPLA). By spectrally slicing and externally injecting the side-mode of such an AR-FPLA, the parameters of the front-facet reflectivity, the injection-locking range, the spontaneous emission dependent Q-factor, the eye diagram and the bit error rate (BER) are determined and discussed.

II. Experimental Setup

Fig. 1 schematically illustrates a DWDM-PON system based on the side-mode injection-locked AR-FPLAs. A standard FPLD with an integrated optical isolator is employed as the master laser for injection-locking the AR-FPLA with a longitudinal mode spacing of 0.6 nm. The front-facet reflectivity of the

Manuscript received January 04, 2010; revised June 03, 2010; accepted July 12, 2010. Date of publication July 23, 2010; date of current version September 29, 2010. This work was supported in part by the National Science Council, Taiwan, R.O.C. and the Excellent Research Projects of National Taiwan University, Taiwan, under Grants NSC98-2221-E-002-023-MY3, NSC98-2623-E-002-002-ET, and NTU98R0062-07.

G.-R. Lin and Y.-C. Chi are with Graduate Institute of Photonics and Optoelectronics, and Department of Electrical Engineering, National Taiwan University, Taipei 106, Taiwan (e-mail: grlin@ntu.edu.tw).

Y.-S. Liao and H.-C. Kuo are with Department of Photonics and Institute of Electro-Optical Engineering, National Chiao Tung University, Hsinchu 300, Taiwan.

G.-C. Lin and H.-L. Wang are with the Advanced Tech. Laboratory, Telecommunication Laboratories, Chunghwa Telecom Company, Ltd., Taoyuan, 32617 Taiwan.

Y.-J. Chen is with Department of Computer Science and Electrical Engineering, University of Maryland at Baltimore County, Baltimore, MD 21250 USA.

Digital Object Identifier 10.1109/JLT.2010.2060470

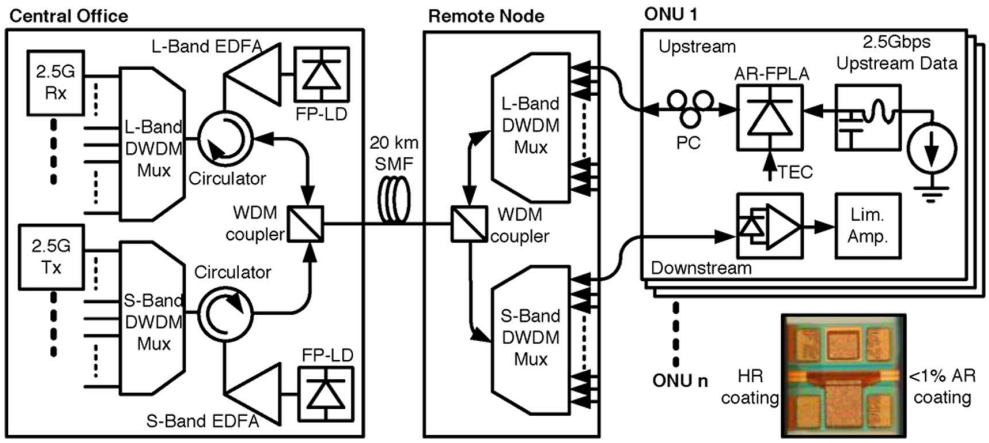

Fig. 1. DWDM-PON system with an AR-FPLA based transmitter at the ONU end that is side-mode injection-locked by a wavelength-sliced master FPLD.

AR-FPLA was coated as low as 1%, and the rear-facet reflectivity was increasing to 99%. Such a highly asymmetric coating allows the efficient injection of ASE, which also reduces undesirable backward reflection at front-facet and avoids the power consumption at rear-facet. To facilitate the injection-locking scheme, the design and fabrication procedures of the AR-FPLA were modified from a conventional FPLD without significantly increasing the production cost. The threshold current of the AR-FPLA is 13 mA. A long-term test of the AR-FPLAs biased at 80 mA and 85°C with output power of 5 mW for more than 4500 hrs was employed for the stable operation of 40 devices used in our experiments.

At the ONU end shown in Fig. 1, each transmitter consists of a polarization controller (PC) that is adjusted to maximize the efficiency of injection from the master FPLD. At the central office, the master FPLD can be replaced by a specially designed long-cavity device with 50-GHz longitudinal mode spacing to match the ITU-T defined DWDM channels. Before injecting into each AR-FPLA at the ONU end, the master FPLD output is channelized by a DWDM multiplexer built-in with the DWDM-PON and amplified by a EDFA (SDO, OAS-1000) with maximum output power of $+18$ dBm, which consequently causes a reduction on threshold current of the slave AR-FPLA. The external injection-locking condition is easily achieved by matching the slave AR-FPLA wavelength with the incoming master signal via a slight temperature and current detuning. The side-mode injection-locked AR-FPLA acts like a single-mode source with high side-mode suppression ratio (SMSR), which is directly modulated by a 2.5-Gbit/s pseudo-random binary-sequence (PRBS) data-stream for transmission performance diagnosis.

The FPLD used in our experiment exhibits a long-cavity to shrink its longitudinal mode spacing to 0.6 nm, which is not coincident with the channel spacing of 50 GHz (or 0.4 nm) set by the AWG based DWDM. The FPLD emits numerous modes before passing through the DWDM, which is filtered into a single-mode spectrum for injection-lock the AR-FPLA afterwards. Technically, the DWDM channels with number of (3n-1) were used in our case. Such a mismatch can be solved by precisely dicing the FPLD chip by the manufacturer.

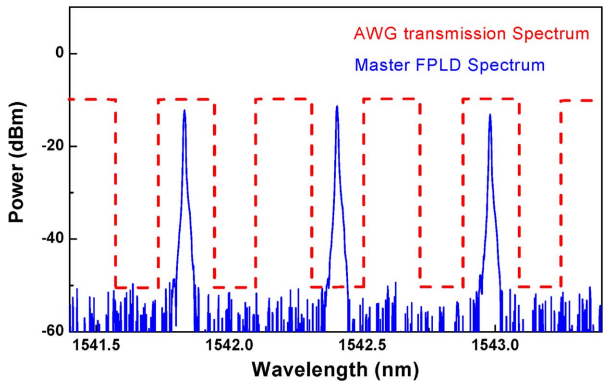

Fig. 2. DWDM-PON system with an AR-FPLA based transmitter at the ONU end that is side-mode injection-locked by a wavelength-sliced master FPLD.

III. Results and Discussions

In comparison with conventional FPLDs, the mode spacing of the AR-FPLA is reduced to ensure that the injected narrowband ASE can spectrally overlap with at least one lasing mode of the AR-FPLA. Such a design easily maintains the wavelength locking regardless of the thermally drifting wavelength of the AR-FPLA modes. The channel spacing of the arrayed waveguide gratings (AWGs) based DWDM multiplexer and demultiplexer nearly rectangular passband shape was chosen to fit the mode spacing of the AR-FPLA. Fig. 3 shows the optical spectrum of the free-running AR-FPLA at biases of 20, 30, and 40 mA. A less distinct and broadened longitudinal mode response can be observed from the AR-FPLA output when biasing below 30 mA. The FWHM of the free-running AR-FPLA output spectrum remains as large as 35 nm even at biased current up to 40 mA. Note that there is still a weak Fabry–Perot effect in the AR-FPLA chip but the major lasing peak is relatively hard to be built up without external injection. After injecting with the spectrally sliced master FPLD signal, the AR-FPLA reveals a perfectly injecting-locking peak with SMSR up to 40 dB (see Fig. 3).

The AR-FPLA exhibits a wide injected-locking range from 1510 nm to 1540 nm at low biased current, which can extend to the S-band if the AR-FPLA bias further enlarges up to 40 mA. As the wavelength of one longitudinal mode in AR-FPLA

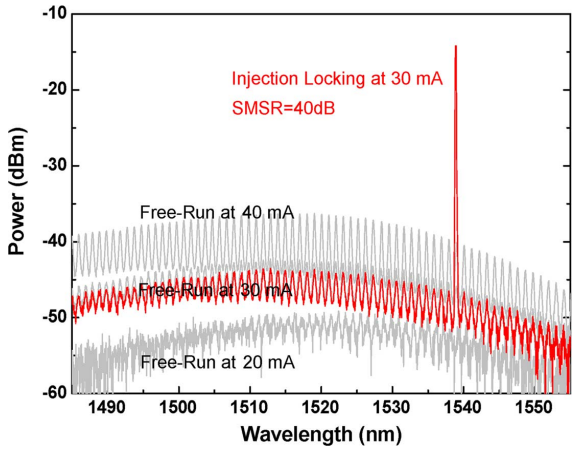

Fig. 3. Output optical spectra of the free-running and injection-locking AR-FPLA at different biased conditions.

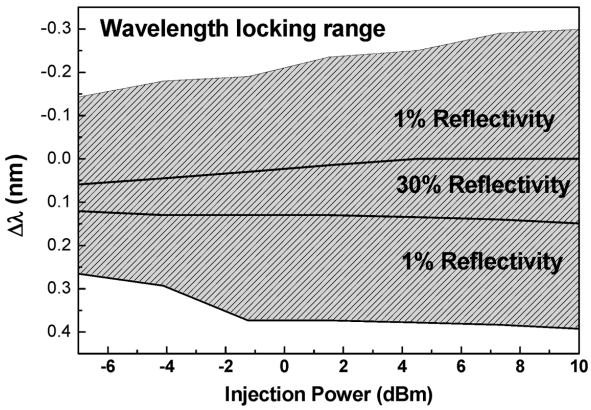

Fig. 4. Injection-locking power dependent wavelength lock-in range of one longitudinal mode in the slave AR-FPLA transmitter at the ONU end.

exactly coincides with that of the incoming FPLD source, the AR-FPLA output the largest peak power with lowest noise. The detuning wavelength is the wavelength shift of the injected signal from the master FPLD with respect to the free-running wavelength of one longitudinal mode of the slave AR-FPLA. As a result, the wavelength locking range of the slave AR-FPLA measured by adopting the modified delaying self-homodyne (MDSH) scheme is shown in Fig. 4. The locking range was defined as the wavelength tunable range needed for retaining the SMSR of the AR-FPLA lasing mode at > 35 dB. The stable lock-in region for injection-locking one longitudinal mode is found to be bounded by two solid curves shown in Fig. 4.

Under a low-level injection condition, a broadened lock-in range for each longitudinal mode is observed for the AR-FPLA as compared to that of the standard FPLD with front-facet reflectivity of 30%. A relatively weak injection-locked signal with considerable noise has also been found even the injecting wavelength is detuned away from the slave AR-FPLA's longitudinal mode by 0.6 nm. The lock-in range of AR-FPLA is greatly increased to be 7–8 times larger than that of a standard FPLD at extremely high bias. Such a less tolerant injection-locking performance essentially benefits the easier lock-in of AR-FPLA from worse wavelength mismatching condition. The wide lock-in range greatly release the need of any restorable wavelength locker set for the commercial FPLD based up-stream transmitter. Moreover, the maximum side-mode injected-locking range of up to 45 nm was limited by the gain profile of the AR-FPLA.

In more detail, the injection-locking dynamics of the AR-FPLD under external injection can be described with the following rate equations. A traveling-wave rate-equation model [12], [13] is constructed to simulate the gain profile of AR-FPLA initiated from the amplified spontaneous emission (ASE). In particular, the opposite-direction parts of the traveling-wave equations are neglected due to the unidirectional propagation of light in AR-FPLA with high reflectivity at the rear facet. Both the ASE and injection locking induced gain-depletion effects are considered, and the asymmetric gain characteristic is also taken into account during simulation. The differential rate equation of carrier density (denoted as dN/dt) and the propagation equations which describe the time-varied powers of the injection-locked AR-FPLA (denoting as dP_λ/dt and $dP_{\lambda i}/dt$) are listed as below

$$\frac{dN}{dt} = \frac{I}{qV} - \frac{N}{\tau_C} - \Gamma v_g g(\lambda_0)(N - N_0)P_{\lambda_0} - \sum_i \Gamma v_g g(\lambda_i)(N - N_0)P_{\lambda_i}, \tag{1}$$

$$\frac{dP_{\lambda_0}}{dt} = \Gamma v_g g(\lambda_0)(N - N_0)\left[(P_{\text{int}} + P_{\text{ext}}) + \frac{h\omega n_{\text{sp}}}{2\pi\tau_c}\right] \tag{2}$$

$$\frac{dP_{\lambda_i}}{dt} = \Gamma v_g g(\lambda_i)(N - N_0)\left[P_{\text{int}} + \frac{h\omega n_{\text{sp}}}{2\pi\tau_c}\right] \tag{3}$$

where I is the injection current, V is the volume of AR-FPLA, q is the electron charge, $\hbar\omega$ is the photon energy, v_g is the group velocity, w is the angular frequency, g (λ) is the gain coefficient, Γ is the optical confinement factor, h is the Planck's constant, P_{int} is the internal photon density, P_{ext} is the external injection photon density, and n_{sp} is the photon number of spontaneous emission. The spontaneous emission lifetime is defined as $\tau_c = (\text{A} + \text{BN}_j + \text{CN}_j^2)^{-1}$ with A, B, and C coefficients denoting the nonradiative, bimolecular, and auger recombination coefficients, respectively. In (2), the last term of $\Gamma v_g g(\lambda)(N - N_0)h\omega n_{\text{sp}}/2\pi\tau_c$ denotes the spontaneous emission noises in AR-FPLA. The solution of these rate equations is numerically solved by the fourth-order Runge–Kutta method.

A Lorentzian gain shape function is employed to describe the spectral roll-off of the AR-FPLA gain profile by $g(\lambda, N) = g_0(1 + ((\lambda - \lambda_0)/\Delta\lambda_{\text{g}})^2)$, where $\Delta\lambda_g = 40$ nm is assumed as the gain bandwidth. If we consider that only the free-running ASE and the external injection are propagated in the injection-locked AR-FPLA, the power gain of the AR-FPLA lasing mode spectrum by involving the weak Fabry–Perot etalon effect happened in the AR-FPLA can thus be modified as

$$E_T = E_0 t_1 e^{gd} r_2 e^{gd} + E_0 t_1 r_2 e^{2gd} + \cdots = \frac{E_0 r_2 t_1^2 e^{2gd}}{1 - r_1 r_2 e^{2gd} e^{i\delta}}, \tag{4}$$

$$I_T = I_0 G(\lambda) = I_0 e^{g(\lambda,N)d}\left[\frac{\frac{1-R_1}{\left(1-\sqrt{R_1R_2}e^{g(\lambda,N)d}\right)^2}}{1 + \frac{4\sqrt{R_1R_2}e^{g(\lambda,N)d}}{\left(1-\sqrt{R_1R_2}e^{g(\lambda,N)d}\right)^2}\sin^2\frac{\lambda\pi}{\Delta\lambda_m}}\right] \tag{5}$$

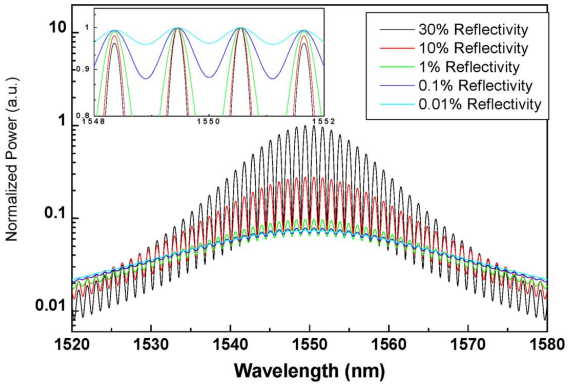

Fig. 5. Simulation of the normalized free-running spectra of AR-FPLA with front-facet reflectivity of 30%, 10%, 1%, 0.1% and 0.01%.

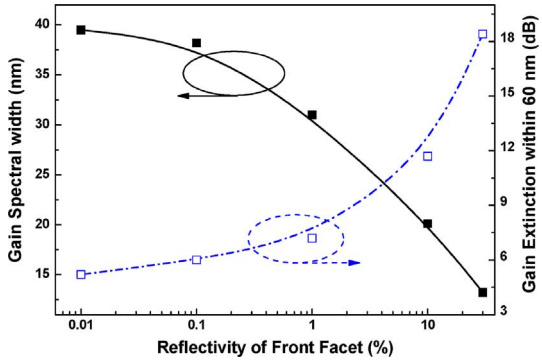

Fig. 6. Gain spectral linewidth (solid squares) and the gain extinction (hollow squares) versus the front-facet reflectivity of AR-FPLA.

where $\delta = (2\pi/\lambda)2nL$, $\Delta\lambda_{\rm m} = \lambda^2/2nL$, $\rm R_1$ and $\rm R_2$ are the reflectivity of the front and rear facets, respectively. The simulated gain spectral profiles for the AR-FPLA with different front-facet reflectivity are illustrated in Fig. 5, which are obtained by assuming the gain of AR-FPLA is equivalent to the loss of cavity at threshold condition, the output power of AR-FPLA is 0.5 mW under the injection, the cavity length (L) is 600 μm, and the refractive index (n) is 3.5. The rear-facet reflectivity ($\rm R_2$) is assumed to be a 100% perfect reflection, whereas five AR-coated front-facet reflectivity of $\rm R_1 = 30\%, 10\%, 1\%, 0.1\%$ and 0.01% are employed for simulation.

In our experiments, the AR-FPLA with end-face AR coating reflectance is only 1%. To our best knowledge, the ultralow facet reflectance below 0.1% cannot be reached by only implanting an AR-coating on the facet of a FPLD. The extremely low facet reflectance ($\rm R < 10^{-5}$) has been demonstrated in commercially available RSOA product (CIP, SOA-RL-OEC-1550) [14], which is approached by concurrently designing an angled facet SOA facet and depositing an AR coating to minimize the end-face reflectance. In principle, a perfect RSOA with an $\rm R_1$ of $< 0.01\%$ can perfectly achieve color-free operation due to its reflectless cavity and mode-free gain spectrum. As compared with other simulated gain spectra, the ROSA with a front-facet reflectivity of 0.01% and 0.1% exhibit similar flattened gain profiles with a spectral linewidth of 39.5 nm and a smallest gain extinction ratio of < 3.3 dB within 60 nm range, as shown in Fig. 6. The simulation supports that the AR-FPLA with front-facet reflectivity of $< 0.5\%$ benefits from more injection-locked channels. The simulating results also show that the longitudinal modes with a relatively large mode extinction ratio (> 2 dB) occurs when coating the AR-FPLA front-facet with 1% reflectivity. Without greatly sacrificing the linewidth of gain spectrum, such an AR-FPLA benefits from a weak Fabry–Perot etalon effect with a slightly larger efficiency at the central gain peak in comparison with the standard RSOA with front-facet reflectivity of 0.01%. As shown in Fig. 6, the simulated gain-spectral linewidth and gain extinction ratio for the 1% front-facet-reflectivity coated AR-FPLA are 32 nm and 7 dB, respectively.

Numerous WDM-PON works have previously emerged with the spectral-sliced ASE injection-locking of RSOA transmitters. However, the spectrum-sliced ASE injection is a detrimental source to the RSOAs or FPLDs due to its relatively large intensity noise and randomized polarization characteristics. Although the ASE injection-locking technique supplies a broadband incoherent light source for multi-channel injection, such an approach usually exhibits high intensity noise to limit its data rate at < 1.25 Gbit/s. To enhance the transmission performance, we employ a master FPLD in front of the EDFA to change the broadband light source from incoherent to coherent. The FPLD-EDFA link plays the role of a multi-channel coherent source to avoid the drawback of an excessive intensity noise generated from the ASE-ASE beating accompanied with the broadband incoherent source. Typically, the spectrally sliced ASE source contains a RIN of -100 dB/Hz to limit the modulation bandwidth of the injection-locked FPLD or AR-FPLA. In contrast, the filtered single-mode-sliced FPLD amplified by EDFA can provide a RIN as low as -135 dB/Hz, which facilitates a lower BER and a better transmission performance in WDM-PON system. In comparison with the spectrum-sliced ASE source, the high-frequency intensity noise of the FPLD injection-locked AR-FPLA can be efficiently suppressed, thus providing a better signal-to-noise (SNR) performance than the spectrum-sliced ASE source for gigabit data transmission in WDM-PON. By modifying the signal-to-noise ratio (SNR) previously demonstrated for an optical transmitter [15], the SNR of the AR-FPLA transmitted data-stream can be correlated with the amplified spontaneous emission of the AR-FPLA by

$$\mathrm{SNR} = G(\lambda)\frac{P_{\rm ext}}{P_{\rm noise}} = \frac{\frac{1-R_1}{\left(1-\sqrt{R_1}\sqrt{R_2}e^{g(\lambda,N)}\right)^2}}{\frac{h\omega n_{\rm sp}}{2\sqrt{2}\pi\tau_c}\left[1+\frac{4\sqrt{R_1}\sqrt{R_2}e^{g(\lambda,N)}}{\left(1-\sqrt{R_1}\sqrt{R_2}e^{g(\lambda,N)}\right)^2}\sin^2\frac{\lambda\pi}{\Delta\lambda_m}\right]}. \quad (6)$$

With the modified SNR model, the measured BER of the data-stream received by the AR-FPLA can also be accurately calculated from the simulated Q factor of the received eye pattern at a desired data rate. Fig. 7 shows the calculated Q factor and locking range of the injection-locked AR-FPLA with different front-facet reflectivity.

In order to evaluate the effects of optical signal performance, intensity noise, and phase noise, the frequency detuning characteristic of the 1% AR-FPLA and 30% FPLD were measured and shown as below. By injecting the optical power of $+3$ dBm, -3 dBm, and -9 dBm, the measured BER of the optical transmitting eye diagram performance can be correlated with the

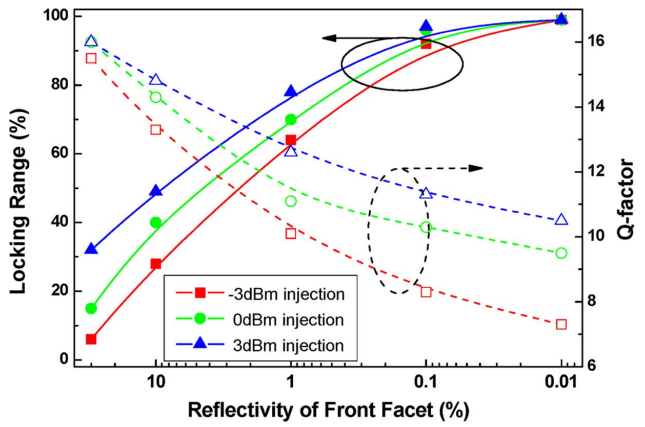

Fig. 7. Calculated Q factor and locking range of the injection locking AR-FPLA with different reflectivity and injection power.

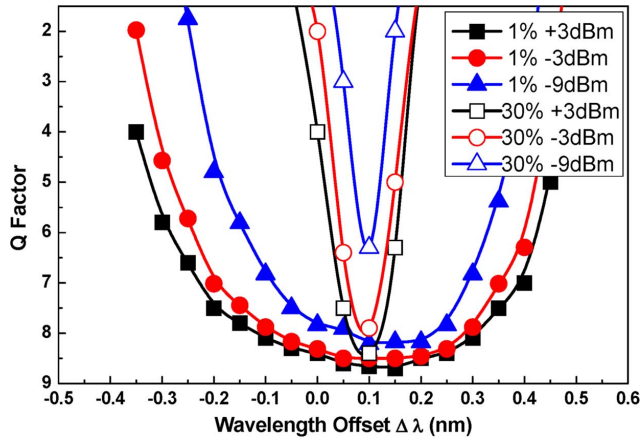

Fig. 8. Q-factors of 1-% reflectivity AR-FPLA and 30-% reflectivity FPLD with injection power of $+3$ dBm, -3 dBm, -9 dBm.

recorded Q factor according to the calculation given by Bergano *et al.* In principle, the signal-to-noise ratio can be measured at the decision circuit of an optical transmission system [15], which is described as $\mathrm{Q} = (\mathrm{I}_1 - \mathrm{I}_0)/(\sigma_1 + \sigma_0)$ and $\mathrm{BER} = 0.5\mathrm{erfc}(Q/2^{0.5})$, where $\mathrm{I}_{1,0}$ denote mean amplitudes of on-level and off-level bit-stream, $\sigma_{1,0}$ the corresponding standard deviation of the marked optical signal rail, and erfc(x) the complementary error function. When comparing with a commercial FPLD with 30% end-facet reflectance, the AR-FPLA shows a great tolerance on the injection-locking wavelength range. Even with an injection power of -3 dBm, the AR-FPLA still exhibits a locking range as wide as 0.48 nm for maintaining the Q factor higher than 7.2 requested for $\mathrm{BER} < 10^{-12}$. The injection locking range is significantly reduced as 0.34 nm while the optically injecting -9 dBm signal. The transmission performance is not affected too much when attenuating the injection level from $+3$ dBm to -3 dBm. With detuning injection wavelength (frequency), the performances of the 2.5 Gbps data transmitted by the AR-FPLA exhibits some degradation. For example, the relative intensity noise (RIN) and the phase noise are inevitably increased from -129 dB/Hz to -120 dB/Hz and from -103 dBc/Hz to -97 dBc/Hz, respectively, when offsetting the $\Delta\lambda$ from 0.1 nm to 0.3 nm. This results in the degradation on calculated Q factor from 8.5 to 8.1 at central wavelength, giving rise to a receiving power penalty of 0.4 dB at BER of 10^{-12}.

According to the simulations, a higher front-facet reflectivity could result in a larger Q-factor to guarantee the transmission of good-quality data-stream at the expense of a narrower locking range as well as a smaller side-mode quantity. The shrinkage on locking range arises from the failure of gain competition when detuning the injection wavelength away from the gain peak of the etalon cavity with restrained optical confinement factor. The front-facet reflectivity of the AR-FPLA should be slightly reduced in order to promote the side-mode injection-locking flexibility of the AR-FPLA. With lowest front-facet reflectivity ($\mathrm{R} = 0.01\%$) and weak injection (-3 dBm), the worst Q factor can still be as high as 7.2 to provide a theoretically predicted BER reaching 1.1×10^{-12} at a data rate of 2.5 Gbit/s. In practical design of the AR-FPLA with $\mathrm{R}_1 = 1\%$, the error-free transmission with $\mathrm{BER} < 10^{-12}$ is easily obtainable since the evaluated Q factor is already larger than 9.5 dB even at a low injection level

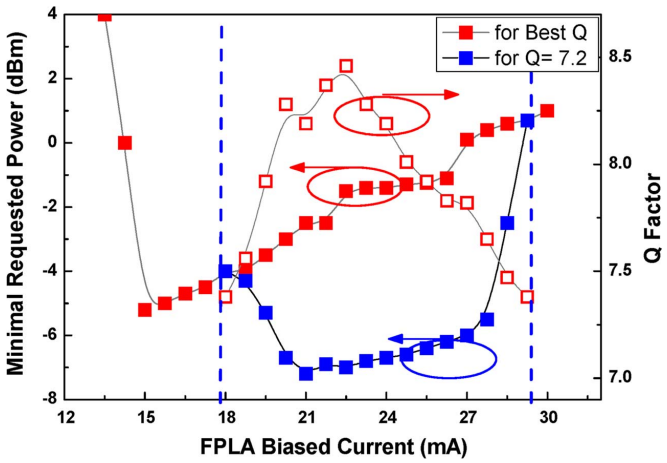

Fig. 9. Requested injecting power (red solid square), corresponding the measured best Q-factor (red hollow square), and the minimal requested injecting power for $\mathrm{Q} = 7.2$ (blue solid square) at different driving currents.

of -3 dBm. In Fig. 9, the Y axis of injecting power denotes the requested optical power for the best Q factor and error-free eye diagram. The best Q factor as high as 8.5 can only be reached by operating the AR-FPLA at 22 mA with optical injection level of -1 dBm at least. The maximum obtainable Q factor and the requested injection power are shown as the hollow- and solid-square curves, respectively. In a practical application, the Q factor minimum requested for standard data-communication with BER under 10^{-12} is only 7.2, which greatly releases the operating conditions of the AR-FPLA for approaching an extremely high Q factor. In order to keep the BER performance at different biased conditions of the AR-FPLA, the minimum injection power required to maintain the Q factor of transmission data above its marginal value (fixing $\mathrm{Q} = 7.2$ at all biased condition) is measured and plotted as the blue-square curve in Fig. 9. In comparison with the operating conditions for best Q factor obtained at biased current of 22 mA, it is observed that only an optical injection power of -6.9 dBm is required to achieve the Q factor of 7.2.

As the bias current increases beyond 22 mA, the larger intra-cavity carrier density forces the AR-FPLA to fix its lasing wavelength at preferred mode, thus the injection-locking can

only be achieved by externally feeding a higher photon density into the AR-FPLA cavity. As a result, the AR-FPLA needs a higher injection power to obtain single-wavelength output and to optimize Q-factor and eye-diagrams. The minimum requested power need to be increased at higher biased current at a fixing Q of 7.2, which is a tradeoff between the gain depletion and the noise suppression for the single-mode injection-locked AR-FPLA or FPLD typically used in the WDM-PON architectures. Therefore, the power budget in our system could be considered to allow an additional 11-dB loss for the whole WDM-PON link, including the fiber loss of 5 dB, the AWG loss of 15 dB, the WDM coupler loss of 2 dB, and the circulator loss of 1 dB. As the minimum required injection power is as low as -7 dBm (at $\mathrm{I_{bias}} = 21$ mA), the required maser FPLD power for such a 32-channel WDM-PON can be estimated to be about 16 dBm after EDFA. By taking the AR-FPLA with its farthest side mode injection-locked by the incoming FPLD signal as an example, the Q factor of the injection-locked AR-FPLA transmitted data-stream can reach 8.5 under a biased current of 30 mA and an injection power below -1 dBm. Even setting the dc biasing current of the slave AR-FPLA as low as 20 mA, the data transmission of AR-FPLA with a Q-factor > 6.0 at data rate > 2.5 Gbit/s can be achieved by injection-locking farthest side-mode, corresponding to a reachable BER of 10^{-9}. On the other hand, the actual injecting level requested for the AR-FPLA injection-locked at different side-modes is strongly dependent with the transient gain contribution of the side-mode in the AR-FPLA. It is clearly seen that the requested injecting power level for obtaining highest Q factor show an inverse hyperbolic function with increasing AR-FPLA bias. At AR-FPLA bias higher than 24 mA, the requested injecting level oppositely decreases from $+1$ to -1 dBm. That is, the optimized operating current of the AR-FPLA for concurrently achieving high-Q (> 7.2) and low-injection (< 0 dBm) are determined as 25 ± 2 mA.

At last, the data transmitting performance of the directly modulated AR-FPLA with its side-mode injection-locked by a filtered FPLD source in a simulated 2.5-Gbit/s WDM-PON system is characterized. Previously, the FPLD wavelength-locked by the spectrum-sliced incoherent light source has been investigated for low-capacity WDM-PON realization, which unfortunately exhibits a limited data rate at 622 Mbit/s for a single channel due to its relatively high RIN. The similar WDM-PON transmitter based on the directly modulated RSOA operating in linear regime has also been proposed with allowable extinction ratio (ER) less than 3 dB [3], [10]. In comparison, the clear eye diagram of the AR-FPLA transmitted data with high extinction ratio (> 8 dB) can be obtained, as shown in the inset of Fig. 10. The rising time and falling time (defined as the duration between 20% and 80% of on-level amplitude) are 118 ps and 125 ps, respectively. By injection-locking the central mode, a nearly error-free ($\mathrm{BER} < 10^{-12}$) back-to-back transmission of the AR-FPLA carried Pseudo Random Binary Sequence (PRBS) data-stream with pattern length of a $2^{31} - 1$ can be detected at receiving optical power of -24.4 dBm. In comparison with a free-running AR-FPLA based transmitter, a negative receiving power penalty is observed for detecting the data-stream with BER of less than 10^{-12}, which is due to the relaxation on the relaxation oscillation and the increasing bandwidth of the

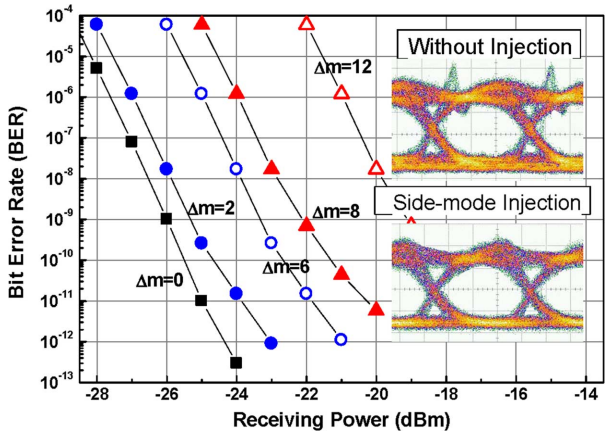

Fig. 10. BER analysis of wavelength injection locked 1% AR-FPLA at different longitudinal modes and measured eye diagrams (inset) with and without injection.

AR-FPLA after injection-locking. Alternatively, if the farthest side-mode (the 12th modes away from the central mode) of the AR-FPLA is injection-locked, the receiving sensitivity at BER of 10^{-12} dramatically degrades to -17.4 dBm with a power penalty of 7 dB, which is mainly attributed to the greatly reduced SNR of the side-mode injection-locked AR-FPLA. For practical application of being the universal ONU transmitter in the WDM-PON system, nearly 17 modes of the AR-FPLA can be used to achieve a data communication with $\mathrm{BER} < 10^{-9}$ at receiving power of larger than -22 dBm at 2.5 Gbit/s. At same BER criterion, there are at least 25 side modes applicable for data transmission with their maximum receiving sensitivity degrading to -19 dBm.

The overshooting effect on the rising edge of on-bit data can be eliminated by stabilizing the gain of AR-FPLA via the assistance of external optical injection. As the transient current changes from bit "0" to bit "1", the damping effect on photon density of the injection-locked longitudinal mode diminishes due to external injection-locking operation, since incoming photons are incorporated with those of the injection-locked longitude mode to equivalently offset the biased point of AR-FPLA beyond its threshold. The threshold current reduction phenomenon of a laser diode under externally optical injection was previously demonstrated by Chang *et al.* [16]. In principle, the threshold current is a nonlinear function of the external injection power or photon density, as described by

$$\begin{aligned} I_{\mathrm{th,ui}} &= \frac{qV}{\eta_i \tau} n_{\mathrm{th,ui}} = \frac{qV}{\eta_i \tau}\left(\frac{g_{\mathrm{th}}}{a} + n_{\mathrm{tr}}\right) \\ &\quad - \frac{qV}{\tau \eta_i a}\left(\frac{R_{\mathrm{sp}}}{S_B} + \sqrt{\frac{4\alpha^2}{(1+\alpha^2)}}\sqrt{S_i}\right) \\ &= I_{\mathrm{th,\ free-running}} - \Delta I_{\mathrm{injection}} \end{aligned} \tag{7}$$

where q denotes the unit charge of a electron, V the volume of the active region, η_i the internal quantum efficiency, τ_{eth} the carrier lifetime at threshold, $\mathrm{N_{th,ui}}$ the carrier number in the active region, $\mathrm{g_{th}}$ the gain at threshold condition, a the differential gain coefficient, $\mathrm{n_{tr}}$ the carrier density at transparent condition, R_{sp} denotes the spontaneous emission rate, S_B the maximum

photon number in the locked mode, α the linewidth broadening factor, k_c the coupling coefficient, and S_i the photon number injected into the laser diode cavity. As a result, the P-I curves of our AR-FPLA sample reduces threshold current obtained by increasing the optical injection power. Obviously, the lower reflectivity on the emitting face can improve the coupling efficiency of optical injection and enhance the corresponding effect. On the other hand, the threshold current reduction significantly affects the damping and the relaxation oscillation of the laser which can be described by modifying a set of regular rate equations with external injection term as below

$$\begin{cases} \frac{dN}{dt} = \frac{I}{qV} - \frac{N}{\tau_{\rm eth}} - \nu_g g(N)(S_B + S_i) \\ \frac{dS_B}{dt} = \Gamma \nu_g g(N) S_B - \frac{(S_B+S_i)}{\tau_p} + S_i \end{cases} \tag{8}$$

where Γ denotes the optical confinement factor. By using the nonlinear gain model of $g(N) = \sigma_g(N - N_{\rm tr})/(1 + \varepsilon S)$, the small signal frequency response of laser is given by

$$S(\omega) = \frac{\Gamma \nu_g \sigma_g S_B \frac{i(\omega)}{qd}}{\left(\frac{\varepsilon S_B}{\tau_{\rm eth}\tau_p} + \omega_r^2\right) - \left(\tau_p + \frac{\varepsilon}{\nu_g \sigma_g}\right)\omega_r \omega - (1 + \varepsilon S_B)\omega^2} \tag{9}$$

where d denotes the thickness of active region. The normalized transfer function, $\mathrm{H}(\omega) = [\mathrm{S}(\omega)/\mathrm{I}(\omega)]/[\mathrm{S}(0)/\mathrm{I}(0)]$, can be numerically calculated. The (9) results in a proportionality between the relaxation oscillation frequency and the externally injected photon density or the effective bias current, that is, $\omega_{\rm r} \propto (\mathrm{S} + \mathrm{S_i})^{0.5} \propto (\mathrm{I} - \mathrm{I_{th}})^{0.5}$. The simulation of (9) reveals that the damping effect on the $\mathrm{H}(\omega)$ is relatively significant with increasing $\mathrm{I}/\mathrm{I_{th}}$. Similar phenomenon was also observed by Z. Xu *et al.* [11] Under the external injection with a photon density of $\mathrm{S}+\mathrm{S_i}$, the threshold current of the AR-FPLA is shrinking from 13 mA to 8 mA by increasing the optical injection power up to -3 dBm. The $\mathrm{I_{bias}}/\mathrm{I_{th}}$ is dynamically increased from 2.3 to 3.75 to enlarge the relaxation frequency in this case, which effectively suppress the overshooting problem on the rising edge of the optical eye-diagram.

In comparison with the results of ASE light source injected FPLD, the incoherent light injection usually brings a relatively high intensity noise to limit the achievable bit rate or transmission distance. The WDM-PON transmitters based on such an injection source can provide a highest data rate up to 1.25 Gbps with the minimum DWDM channel spacing of 100 GHz. With the use of coherent light source injection, the AR-FPLA based WDM-PON transmitter becomes a potential candidate for achieving 2.5-Gbit/s transmission in DWDM-PON system with channel spacing of 50 GHz. Although a 10-Gbps WDM-PON injected by DFB laser diode was previously demonstrated by Z. Xu *et al.*. [11], which only allows a wavelength-detuning range of 3.6 GHz (0.029 nm) at BER of 10^{-9}. The wavelength matching and temperature controlling circuitry is mandatory for this approach. Since the temperature-dependent wavelength shifting slope of a regular commercial FPLD is 0.06 nm/°C, and the temperature of FPLD with locking range of 0.029 nm should be maintained within ± 0.25°C. This is not an easy approach to deal with the locking range and the BER performance within such a tiny temperature tolerance. There is always a tradeoff between intensity noise and coherence of the injection-locked FPLD or AR-FPLA based transmitters in the WDM-PON architectures. In addition, a slight degradation on the eye-diagram and BER when detuning the polarization state of the external injection to be orthogonal to the preferred polarization state of the AR-FPLA was observed. At free-running case, the requested power of optical injection into the AR-FPLA could be greatly increased due to the deviation of the injected polarization from the preferred state of the AR-FPLA. In practical application, such a problem relies on the self-restoration of the preferred polarization for the injection-locked AR-FPLA, which can be achieved by feedback controlling an electronically tunable polarization controller added prior to the AR-FPLA. Although such a proposed scheme cannot eliminate the common problem on the polarization sensitivity accompanied with the injection-locked FPLD or AR-FPLA, the wavelength locking and polarization matching can be designed within a feedback control loop to implement a practical self-restorable injection locker.

IV. Conclusion

We theoretically and experimentally investigate the effect of the front-facet reflectivity of the AR-FPLA on the injection locking range, the spontaneous emission dependent SNR and Q-factor, and the BER transmission response. The front-facet reflectivity of AR-FPLA is theoretically analyzed to be smaller than 1% in order to obtain a wide gain spectral linewidth and low gain extinction ratio, which benefits from the largest number of injection-lockable side modes. As a result, the 30-nm wavelength-locking capacity of the directly modulated AR-FPLA based ONU transmitter with 1% front0facet reflectivity under side-mode injection-locking condition is demonstrated for 2.5-Gbit/s DWDM-PON application. The largest SMSR up to 40 dB and a least Q factor of 9.5 dB is achieved when injection-locking the central mode with a seeding power level of -3 dBm, which provides a receiving sensitivity of -24.4 dBm at BER of 10^{-12}. Even injecting-locking the farthest lockable side modes of the AR-FPLA can reach a SMAR > 35 dB and a Q factor of 8.5. The maximum usable ONU channels of the side-mode injection-locking AR-FPLA are 25, corresponding to a wavelength locking range of 30 nm. A BER of $< 10^{-12}$ is obtained for the nearest 17 channels with worst receiving sensitivity of -21 dBm, and all of the injection-locked side-modes in the AR-FPLA can reach a BER of 10^{-9}, providing a largest power penalty of 7 dB as compared to the central-mode injection-locking condition. The simulating and experimental results indicate the flexibility and the limitation of the side-mode injection-locked AR-FPLA based transmitter, which can still be a potential candidate of the cost-effective universal ONU transmitter for 2.5 Gbit/s DWDM-PON systems.

References

[1] H. D. Kim, S. G. Kang, and C. H. Lee, "A low-cost WDM source with an ASE injected Fabry-Pérot semiconductor laser," *IEEE Photon. Technol. Lett.*, vol. 12, no. 8, pp. 1067–1069, Aug. 2000.

[2] K. Lee, J.-H. Song, H.-K. Lee, and W.-V. Sorin, "Multistage access network for bidirectional DWDM transmission using ASE-injected FPLD," *IEEE Photon. Technol. Lett.*, vol. 18, no. 5–8, pp. 761–763, Mar.–Apr. 2006.

[3] W. Lee, M.-Y. Park, S.-H. Cho, J. Lee, C. Kim, G. Jeong, and B.-W. Kim, "Bidirectional WDM-PON based on gain-saturated reflective semiconductor optical amplifiers," *IEEE Photon. Technol. Lett.*, vol. 17, no. 11, pp. 2460–2462, Nov. 2005.
[4] P. Healey, P. Townsend, C. Ford, L. Johnston, P. Townley, I. Lealman, L. Rivers, S. Perrin, and R. Moore, "Spectral slicing WDM-PON using wavelength-seeded reflective SOAs," *Electron. Lett.*, vol. 5, no. 19, pp. 1181–1182, Sep. 2001.
[5] K.-M. Choi, J.-S. Baik, and C.-H. Lee, "Color-free operation of dense WDM-PON based on the wavelength-locked Fabry-Pérot laser diodes injecting a low-noise BLS," *IEEE Photon. Technol. Lett.*, vol. 18, no. 9–12, pp. 1167–1169, May–June 2006.
[6] H.-C. Kwon and S.-K. Han, "Performance analysis of a wavelength-locked Fabry–Perot laser diode by light injection of an external spectrally sliced Fabry–Perot laser diode," *Appl. Opt.*, vol. 45, no. 24, pp. 6175–6179, Aug. 2006.
[7] D. J. Shin, D. K. Jung, H. S. Shin, J. W. Kwon, S. Hwang, Y. Oh, and C. Shim, "Hybrid WDM/TDM-PON with wavelength-selection free transmitters," *J. Lightw. Technol.*, vol. 23, no. 1, pp. 187–195, Jan. 2005.
[8] X. J. Meng, T. Chau, and M. C. Wu, "Improved intrinsic dynamic distortions in directly modulated semiconductor lasers by optical injection locking," *IEEE Trans. Microw. Theory Tech.*, vol. 47, no. 7, pp. 1172–1176, Jul. 1999.
[9] G.-R. Lin, Y.-H. Lin, and Y.-C. Chang, "Theory and experiments of a mode-beating noise-suppressed and mutually injection-locked Fabry-Pérot laser diode and erbium-doped fiber amplifier link," *IEEE J. Quantum Electron.*, vol. 40, no. 8, pp. 1014–1022, Aug. 2004.
[10] S.-M. Lee, K.-M. Choi, S.-G. Mun, J.-H. Moon, and C.-H. Lee, "Dense WDM-PON based on wavelength-locked Fabry-Pérot laser diodes," *IEEE Photon. Technol. Lett.*, vol. 17, no. 7, pp. 1579–1581, Jul. 2005.
[11] Z. Xu, Y.-J. Wen, W.-D. Zhong, C.-J. Chae, X.-F. Cheng, Y. Wang, C. Lu, and J. Shankar, "High-speed WDM-PON using CW injection-locked Fabry-Pérot laser diodes," *Opt. Exp.*, vol. 15, pp. 2953–2962, 2007.
[12] K.-Y. Park, S.-G. Mun, K.-M. Choi, and C.-H. Lee, "A theoretical model of a wavelength-locked Fabry-Pérot laser diode to the externally injected narrowband ASE," *IEEE Photon. Technol. Lett.*, vol. 17, no. 9, pp. 1797–1799, Sep. 2005.
[13] G.-R. Lin, Y.-S. Liao, and G.-Q. Xia, "Dynamics of optical backward-injection-induced gain-depletion modulation and mode locking in semiconductor optical amplifier fiber lasers," *Opt. Exp.*, vol. 12, no. 10, pp. 2017–2026, May 2004.
[14] P. Healey, P. Townsend, C. Ford, L. Johnston, P. Townley, I. Lealman, L. Rivers, S. Perrin, and R. Moore, "Spectral slicing WDM-PON using wavelength-seeded reflective SOAs," *Electron. Lett.*, vol. 37, pp. 1181–1182, 2001.
[15] N. S. Bergano, F. W. Kerfoot, and C. R. Davidsion, "Margin measurements in optical amplifier system," *IEEE Photon. Technol. Lett.*, vol. 5, no. 14, pp. 304–306, Jul. 1992.
[16] Y.-C. Chang, Y.-H. Lin, J. Chen, and G.-R. Lin, "All-optical NRZ-to-PRZ format transformer with an injection-locked Fabry–Perot laser diode at unlasing condition," *Opt. Exp.*, vol. 12, pp. 4449–4456, 2004.

Gong-Ru Lin (S'93–M'96–SM'04) received the B.S. degree in physics from Soochow University, Taipei, Taiwan, in 1990, the M.S. and the Ph.D. degrees in electro-optical engineering from National Chiao Tung University, Hsinchu, Taiwan, in 1990 and 1996, respectively.

He was the faculty member of several universities in Taiwan from 1997 to 2006. He joined the Graduate Institute of Photonics and Optoelectronics (GIPO) and the Department of Electrical Engineering in National Taiwan University (NTU) a full professor since 2006. He is currently directing the Laboratory of Fiber Laser Communications and Si Nano-Photonics in GIPO, NTU, Taiwan. He is the Member of OSA, the Senior Member of IEEE, the Fellow of SPIE, the Fellow of IET, and the Fellow of IOP. He is currently the Deputy Chair of GIPO in NTU and the Chair of IEEE/Photonics Taipei Chapter. He has co-authored more than 150 SCI-ranked journal papers and 200 international conference papers during his research career. His research interests include the fiber-optic communications, the all-optical data processing, the femtosecond fiber lasers, the nanocrystallite Si photonics, the ultrafast photoconductors and the optoelectronic phase-locked loops.

Yu-Sheng Liao received the B.S. dual degrees in applied mathematics (AM) and electrical engineering (EE) from the National Chiao Tung University (NCTU), Taiwan, in 2002. He is currently a Ph.D. candidate in Department of Photonics and Institute of Electro-Optical Engineering at National Chiao Tung University (NCTU).

He has (co)authored more than 12 papers in international periodicals and over 25 papers in international conferences, and his researching interests include fiber-optic communications, all-optical data processing, and millimeter-wave photonic phase-locked loops.

Yu-Chieh Chi was born in Taipei, Taiwan, in 1983. He received the B.S. degree from the Department of Electrical Engineering (EE), National Taipei University of Technology (NTUT), Taiwan, in 2005, the M. S. degree from Department of Electro-Optical Engineering, NTUT. He is currently a Ph.D. candidate in Graduate Institute of Photonics and Optoelectronics at National Taiwan University (NTU).

Hao-Chung Kuo (S'98–M'99) received the B.S. degree in physics from the National Taiwan University, Taipei, Taiwan, R.O.C., in 1990, the M.S. degree in electrical and computer engineering from Rutgers University, New Brunswick, NJ, in 1995, and the Ph.D. degree in electrical and computer engineering from the University of Illinois-Urbana Champaign in 1999.

He has an extensive professional career, both in research and industrial research institutions, which includes the following: Research Consultant in Lucent Technologies, Bell Labs (1995–1997); R&D Engineer in the Fiber-Optics Division at Agilent Technologies (1999–2001); and R&D Manager in LuxNet Corporation (2001–2002). In 2002, he joined the National Chiao-Tung University as a Faculty member of the Institute of Electro-Optical Engineering. His current research interests include the epitaxy, design, fabrication, and measurement of high-speed InP- and GaAs-based vertical-cavity surface-emitting lasers, as well as GaN-based light-emitting devices and nanostructures. He has authored and coauthored 140 internal journal papers, 2 invited book chapter, 6 granted and 10 pending patents.

Gong-Cheng Lin was born in Kaohsiung, Taiwan, in 1971. He received the B.S. degree in mechanical engineering from Chung Hua University, Taiwan, in 1996, and the M.S. degree in electro-optical engineering from Tatung University, Taiwan, in 2001.

Currently, he is an Associate Researcher with the Telecommunication Laboratories Advanced Technology, Chunghwa Telecom Co., Ltd. His research focuses on semiconductor devices packaging, and WDM-PON optical networks.

Hai-Lin Wang was born in Taiwan, in 1961. She received the B.S. and M.S degrees in material science and engineering from National Tsing Hua University, Hsinchu, Taiwan, in 1983 and 1986, respectively.

Currently, she is a Researcher with the Telecommunication Laboratories Advanced Technology, Chunghwa Telecom Co., Ltd. Her research focuses on semiconductor devices packaging, fabrication of semiconductor devices, and WDM-PON optical networks.

Yung-Jui Chen (F'00) received the Ph.D. degree of physics from the University of Pennsylvania, Philadelphia, in 1976.

His current research focuses on areas concerning terabit optical network, integrated optics and optoelectronic integrated circuits, optoelectronic material and device physics, biosensors and biomedical engineering, and ultrafast optical and nonlinear optics.

Dr. Chen is a Fellow of OSA.